

# A Convolution of Hybrid Domain Features for Human Recognition from Face Images

JYOTHI KIRAN G C, Assistant Professor, Dept. of Electronics and Communication Engineering,

BMS College, Bengaluru, India, jyothirkk1@gmail.com

Ramachandra A C, Dept. of Electronics and Communication Engineering, NMIT, Bengaluru,

India, ramachandra.ace@gmail.com

K B Raja, Dept. of Electronics and Communication Engineering, University Visvesvaraya College

of Engineering, Bangalore University, Bengaluru, India, raja\_kb@yahoo.com

**Abstract:** The face recognition in biometrics is a challenging task as the variations in facial expressions, illumination, resolution, rotation in the face, and similarities in face structure among persons. In this paper, we propose a Convolution of Hybrid Domain features for human recognition in face images. The benchmarked face images are considered and converted into grayscale and resized to uniform dimensions of 128x128. The Discrete Wavelet Transform (DWT) is applied on face images to compress and to enhance quality of face image. The Histogram of oriented gradients (HOG) is used on a compressed LL band of DWT to extract initial features which are not affected by lighting variations of an image. The LL band of DWT and HOG are connected in cascade by connecting the output of the LL band to the input of HOG. The input and output of HOG are convolved to generate new prominent robust final features. The Euclidean Distance (ED) is used for computing the results of the system on comparing database and test features. It is observed that the results of the proposed system are better than the existing systems.

**Keywords:** Biometrics, Convolution, DWT, ED, Face Recognition, HOG.

## I. INTRODUCTION

Identifying humans in a face images are a challenging assignment due to their adaptable appearance and the varied kind of postures. The face image is a very important communicating tool between humans and machines without touching and contacting physically by maintaining social distance in the applications of public transportation systems, entry into the offices, entry into Hospitals etc., in the present scenario of worldwide COVID 19 Pandemic disease. The primary requirement is a strong feature set that permits the humans to be separated effectively, even in messy backgrounds of face images. Biometrics are developed from ancient history as the supreme guaranteed in recent technique of computerized individual identification entered a new era in security in the world [1,2,3]. The Biometric credentials are based on some physiological traits, viz., a face, palm print, fingerprint or iris pattern, and also on some behavioral traits such as, signature, keystroke or gait [4]. The time domain/spatial domain signals are raw signals, which are converted into other domains to obtain more information for several applications and extract features for biometric recognition. The readily available transformations are Fourier Transform [5], Discrete Fourier Transform [6], Fast Fourier Transform [7,8], Discrete Cosine and Sine Transforms [9] convert time domain/spatial domain into the frequency

domain to obtain frequency components of the signal and does not give the information of time. The limitation of the transformations of not providing frequency components corresponding time, location is addressed by the Wavelet Transform [10]. A range of biometrics application areas electronic gadgets, banking, immigration, law enforcement, telecommunication networks, monitoring the time and attendance of staff, Cloud computing, big data analytics, video analytics, health caring systems, National security systems and many web based applications.

**Contributions:** In this paper, we introduced cascade of DWT and HOG techniques for initial features of face images. The final features are extracted by convolving LL band of DWT and HOG matrices which are predominant and robust features of face images for recognition of humans. The distance measure ED is used to compare database and detect face image features to verify the performance of the proposed method.

**Organization:** The rest of this research paper is arranged as follows. Section II discusses previous works in feature extraction, and classification techniques related to face recognition. Section III discusses the proposed system model. Section IV presents the proposed algorithm, the system's experimental results and comparison with existing techniques

are discussed in the section. Section VI concludes this work with recommendations for future work.

## II. LITERATURE SURVEY

X. Han et al., [11] proposed training single sample per person (SSPP) face recognition system. The technique histograms of oriented gradients (HOG) algorithm are used to calculate the features based on structure of face matrix and Pearson correlation to classify the features with SSPP. The techniques HOG and Pearson correlation sorts effectively differences in face variations, contributes to a good performance in the model. Rajput et al., [12] described the usage of HOG in feature extraction for face recognition. The face images of frontal pose with normal lighting, neutral expression, and no occlusions are considered. The query face image sketch drawn by an artist are considered and applied HOG feature descriptor. The HOGs of artist sketch are calculated and are related against the database face images using KNN classifier. ZXieet al., [13] presented fusion of Local binary pattern (LBP) and HOG based face recognition algorithm. The LBP has limitation in extracting the edge and direction information in face images, hence LBP operator is used to extract the texture feature of face. The edge features of the original infrared face images are extracted by HOG operator. The Multiple Kernel Learning (MKL) is used to combine the texture features and edge features to obtain better features.

Ghorbani et al., [14] proposed HOG and LBP features for face recognition with three main contributions. First, HOG descriptor is used to reduce errors due to occlusions, pose and illumination fluctuations in face images. Second, combination of HOG descriptors at different scales with the LBP to capture vital structure for face recognition. Third, identification of better feature selection to eliminate redundant and unrelated features. H Wang et al., [15] presented a fusion of Local Difference Binary (LDB) and HOG for face recognition. The LDB descriptor is used to extract the local pattern features of a face images. The edge features of the face images are extracted by HOG. The fusion of LDB and HOG features improves the quality of features is high. The experimental results are tested on ORL and Yale face databases. Nhat and Hoang [16] developed fusion of feature sets based on canonical correlation analysis to concatenate different feature sources for face image. The standard descriptors such as LBP, HOG, and GIST are used to extract features based on block division.

Prasetio et al., [17] proposed the approaches for anxiety recognition on three classes viz., neutral, low stress, high stress from a facial frontal images. The face image is divided into three parts such as pairs of eyes, nose, and mouth. The features are extracted from each pair of image using DoG, HOG, and DWT. The strength of orthonormality features is measured by the RICA. The GDA distributes the nonlinear covariance. The histogram features of the image pairs are applied at a depth-based learning of ConvNet to test the

model. Jain et al., [18] aims to detect faces from any given image and extract features from eyes and lips and categorize them into 6 emotions viz., happy, fear, anger, disgust, neutral, sadness. The methods, including passing the training images through Gabor filter, or HOG and DWT for better classification of data are implemented. The better outcome achieved by passing the training images through HOG, followed by SVM. Rangsee et al., [19] proposed a nibble-based face recognition using convolution of hybrid features. The novel technique of converting decimal value of each pixel into 8-bit binary and is split into Left-Side Nibble (LSN) and Right-Side Nibble (RSN) is introduced to increase computational speed. The 4-bit LSN is changed to a decimal value varied between 0 and 240. The DWT is used on LSN matrix and only LL band coefficients are measured as first set of transform domain features. The 4-bit RSN is changed into decimal values ranging between 0 and 15 and HOG is used on RSN matrix to generate second set of spatial domain features. The final features are created by linear convolution on spatial and transform domain features. The Artificial Neural Network (ANN) is used to classify the images.

Zhao Lihong et al., [20] presented face recognition based on Wavelet and Fourier transforms. The features are found by merging DWT with Fourier transform and they are classified by the Nearest-Neighbor classifier with the comparison metric of Euclidean distance and correlation coefficient. Espinosa-Duro and Monte-Moreno [21] described a biometric face identification method based on frontal face images that merges the wavelets theory with the probabilistic neural nets structure. The DWT is used to reduce the dimensionality of the face images, and a radial basis neural net classifier is used for identification process. Atamuradov et al., [22] investigated the performance of proposed system, by adding additive white Gaussian noise to the test images in the face database. The two algorithms DWT and Dual-Tree Complex. Wavelets Transform (DTCWT) are used for de-noising. The de-noised images are then nurtured with PCA-based face recognition for improved results. Lahaw et al., [23] exploited the idea of 2D-DWT for the image compression as a preprocessing in face recognition. The DWT is executed at different scales and placements for sensitive to varying lighting conditions and facial details. The LL sub-band of the processed image is used for feature extraction process with ICA, PCA, LDA and SVM algorithms.

## III. PROPOSED SYSTEM MODEL

This section deals with human recognition using face images by cascading earlier techniques DWT and HOG. The experimental setup to fuse input and outputs of HOG algorithm using convolution is established to extract robust features with the following steps.

### A Face image datasets

The proposed model is tested using regular four different face data sets viz., JAFFE, L-SPACEK, YALE and ORL.

a. Japanese Female Face Expression (JAFFE)

It contains 10 distinct persons and twenty different images for each person totalling to 200 samples of images. The size of every image is 256 x 256 grayscale. The database images were captured with an upright, frontal positions. The figure 1 shows all the images of a single subject which are in tiff format having 7 different emotional facial expressions.

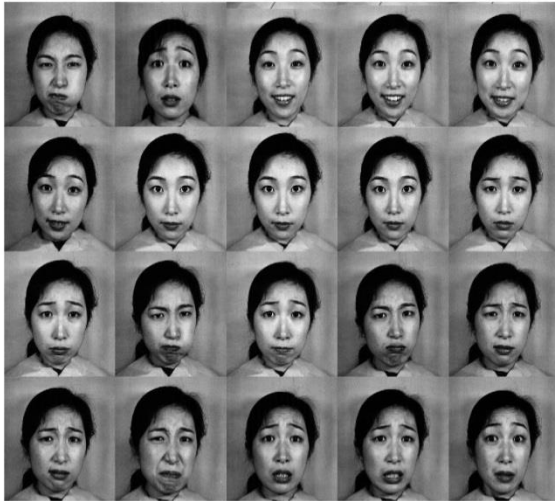


Figure 1. Images of JAFFE data set [24]

b. Libor Spacek's (L-Spacek's) Facial Images Databases

The dataset has totally 3040 images of 152 persons with twenty images per persons. All the images are varied only facial expression on the plain green background with a size of 200X180 in 24-bit GRB image. Figure 2 shows the twenty face image samples of one person.



Figure 2. Twenty L- Spacek's Samples of one person [25]

c. YALE Database

The face images of dissimilar facial expressions such as happy, sad, normal, sleepy, surprised, wink, with glasses, without glasses, center-light, left-light, right-light are captured for every person. The samples of a single person are given in figure 3. The database consists of 15 persons with 11 face image samples from each person. The size of each face image is 320x243 with the GIF format.



Figure 3. Images of Yale database [26]

d. ORL Database

A regular Olivetti Research Laboratory (ORL) face database covers images taken between 1992 and 1994. Ten different facial expressions like open/closed eyes, smiling/not smiling, with/without glasses, varying lightening conditions of single person are captured. Similarly, face images of forty persons were taken under dissimilar conditions. A shady background with upright frontal and slight tilt of the head positions are considered while capturing images. The total number of 400 images of 40 persons is in PGM format and each image size is 92x112. Ten image samples of a single person is shown in figure 4.



Figure 4. ORL samples of single person [27]

B. Preprocessing

The RGB face images are converted into gray scale images for simple and easy processing of images. The grayscale images from different benchmarked face image databases of different dimensions are resized to uniform dimension of 128x128 to extract fixed number of features for all kinds of face databases.

C. Discrete Wavelet Transform (DWT)

The applications are de-noising signals, compressing images, identifying pure frequencies and also used to extract features of biometric traits. This transformation is used to compress face images and also for de-noising. It is a linear transformation in which the basis function wavelet is scaled and shifted version. The wavelet is a small wave of limited duration with an average value of zero. The wavelet transform provides together time and frequency information, which overcome the limitations of other transformations. The wavelet has a variable window width with energy is equally distributed in positive and negative directions. It has band

pass characteristics in the frequency domain as shown in Figure 5 using Low Pass Filter (LPF), and High Pass Filter (HPF) and down sampling of rows and columns of images.

The 2D-DWT signals through sub-band coding for computerized pictures is executed and utilizing sub band examination pictures are extricated in approximate shapes in both horizontal and vertical headings, facts in horizontal heading towards discovery of horizontal edges, specifics in vertical heading towards discovery of vertical edges and specifics in both horizontal and vertical headings towards discovery of diagonal edges. The 2-D signal investigation utilizes taking over 2-D filter tasks complete the increase of distinguishable scaling and wavelet tasks in n1 tests in horizontal and n2 tests in vertical headings as characterized by taking after conditions [28].

For approximate band,

$$\Phi (n1, n2) = \varphi(n1) \varphi(n2) \quad (1)$$

For the horizontal band,

$$\psi^H (n1, n2) = \psi(n1) \varphi(n2) \quad (2)$$

For the vertical band,

$$\psi^V (n1, n2) = \varphi(n1) \psi(n2) \quad (3)$$

For the diagonal band,

$$\psi^D (n1, n2) = \psi(n1) \psi(n2) \quad (4)$$

The sub-sampling filter by a factor of 2 and every sub-band relates to the one-fourth of the input dimensions. The sub-bands viz.,  $\varphi (n1, n2)$ ,  $\psi^H (n1, n2)$ ,  $\psi^V (n1, n2)$  and  $\psi^D (n1, n2)$  are referred to LL, LH, HL and HH correspondingly.

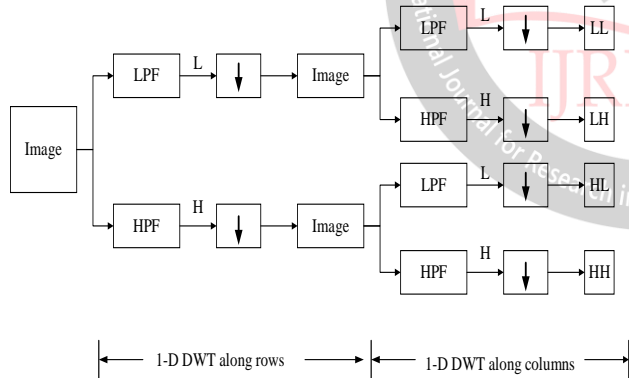


Figure. 5 One level 2D-DWT image decomposition

The LL band is an approximation band consists of low frequency components and has substantial information about the original image. The detailed bands corresponding to high frequency components are LH, HL and HH. The edge information of horizontal, vertical and diagonal are available in LH, HL and HH respectively, which contribute trivial information of an original image. The original image of 128x128 dimension is changed into four sub-bands and each of 64x64 size. In our technique only LL band coefficients of dimension 64x64 are used.

### D Histogram of Oriented Gradient (HOG)

It works on local cells of matrix, which is invariant to geometric and photometric transformations and suitable for human detection in face images [29, 30, 31]. The HOG of LL Sub-band is calculated by horizontal and vertical gradients by the following kernels  $dx$  and  $dy$ .

$$dx = [-1 \ 0 \ 1]$$

$$dy = [-1 \ 0 \ 1]^T$$

For LL band matrix I, the gradients can be computed using convolution operation as given in Equations (5) and (6).

$$I_x = I * dx \quad (5)$$

$$I_y = I * dy \quad (6)$$

The gradient magnitude and directions are calculated using the Equations (7) and (8).

$$\text{Magnitude of gradient} = \sqrt{I_x^2 + I_y^2} \quad (7)$$

$$\text{Angle of gradient} = \arctan(I_y/I_x) \quad (8)$$

The HOG of LL band matrix, is computed by dividing the LL band matrix into 8x8 segments. The angles vary from 0 and 180 degrees instead of 0 to 360 degrees for 8x8 matrix and are unsigned gradients as its negative values are characterized by the similar numbers. The process of calculating the magnitude and direction of the gradient of HOG for the 8X8 area is shown in Figure 6. The bin is selected based on the direction and the value is filled with the magnitude.

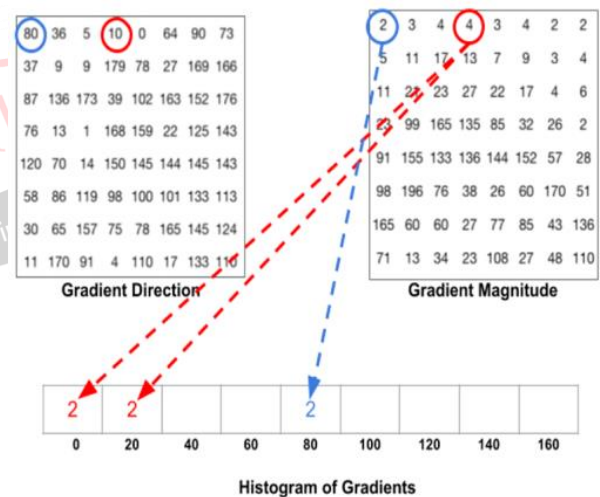


Figure 6. Computation of HOG [32]

All the coefficients in the 8X8 cells are combined to create 9-bin histogram corresponding to directions 0, 20, 40, 60, 80, 100, 120, 140, 160. A bin is selected based on the angle, and the value that goes into the bin is based on the magnitude. The coefficient value circled in blue has an angle of 80 degrees and the corresponding magnitude of 2 is mapped to the 5th bin. The gradient at the coefficient circled using red has an angle of 10 degrees and the corresponding magnitude of 4. Since 10 degrees is half way between 0 and 20, the mapping splits evenly into the two bins of 0 and 20 i.e., 1st and 2nd

bins. The histogram of gradients of all the coefficients in the 8x8 cells are summed up to create the 9-bin histogram. For normalization 16x16 block is used which contains four 8x8 cells, which gives 9x4=36x1 feature vector. The concept L2-Norm of normalization on histogram gradient vector of 39x1 from 16x16 matrix of LL band is used to reduce the effect of variations in illuminations of original face images. For the LL band matrix of size 64x64, total number of 16x16 overlapping (8x8) blocks are 7x7, hence the total number of features are 7x7x36. That means feature vector size is 1764x1. The HOG row histogram vector 1764x1 of LL is converted into matrix. Let first vector  $p_i = [p_1, p_2, p_3, \dots, p_M]$  Let the second vector  $q_i = [q_1, q_2, q_3, \dots, q_M]$  of size 42x42.

**E Convolution [33]**

The convolution among two sets of features is a blend of two kinds of features, yielding a predominantly impressive third set of features in biometric recognition by noise reduction, enhancing edge detection and sharpening. It is the summation of the products of the LL band coefficients and HOG coefficients of LL band after one is reversed and shifted and the summation is evaluated for all values of shift, producing the new convolution result with unique output. The LL band image L (M1, N1) of size 64X64 is convolved with the HOG of LL band matrix H (M2, N2) of size 42X42. The final features of face image are given in equation 9.

$$F(u, v) = \sum_{m=0}^{M_1-1} \sum_{n=0}^{N_1-1} L(m, n) \cdot H(u - m, v - n) \tag{9}$$

Where,  $0 \leq u \leq (M_1 + M_2 - 1)$  and  $0 \leq v \leq (N_1 + N_2 - 1)$

**F Matching [34]**

The Euclidean Distance (ED) is the computation of distance between two points in two vectors to compare similarities and differences between two vectors and is given in equation 10.

Let first vector  $p_i = [p_1, p_2, p_3, \dots, p_M]$   
 Let second vector  $q_i = [q_1, q_2, q_3, \dots, q_M]$

$$D1(p, q) = \sqrt{\frac{1}{M} \sum_{i=1}^M (p_i - q_i)^2} \tag{10}$$

Where M is the dimension of feature vectors,  $p_i$  is the coefficients of database feature vector, and  $q_i$  is the coefficients of the test feature vector.

**IV. PROPOSED ALGORITHM**

**Problem Definition:** Human recognition using face images by cascading DWT and HOG to extract initial features. The input and output of HOG are convolved to extract robust final features to test the performance of the system.

**Objectives:** The goal of the system is to extract robust features of face images from a variety of variations in images. The aim of the system is to recognize humans with 1. High recognition rate 2. Low error rate.

Input: Standard face databases are considered to test the proposed model.

**Output:** The performance parameters are computed to validate the system superiority.

Step 1: The face databases such as JAFEE, L-Space K, YALE and ORL are considered.

Step 2: Pre-processing technique is applied on face images to convert RGB to grayscale images and different dimensions of several face databases are converted into uniform size of 128x128.

Step 3: DWT is applied to pre-processed image to generate low (LL) and high frequency bands

Step 4: HOG is applied to LL band (64x64) of DWT to generate HOG matrix of size 42x42.

Step 5: the DWT and HOG are connected in the form of a cascade. The input (64x64) of HOG and output (42x42) of HOG are convolved to generate final robust features.

Step 6: The distance formula ED is used to calculate performance parameters on comparing database features and test image features.

Step 7: The performance of the system is evaluated by creating databases with different combinations of Persons Inside Database (PID) and Persons Outside Database (POD).

Step 8: The system performance is compared with existing methods to claim superiority of the proposed method.

**V. PROPOSED MODEL IMPLEMENTATION AND ANALYSIS**

In this section, the performance metrics, experimental analysis using four face data sets and comparison of the proposed model with the existing methods are discussed. The values of FAR, FRR, EER, MTSR and OTSR for different combinations of Person Inside Database (PID) and Person Outside Database (POD) are computed and plotted the variations with respect to the threshold values.

**A Performance Metrics**

**a. False Accept Rate (FAR)**

The test image not from the data set is matched with the images in the data set. The FAR can be calculated using Equation 11.

$$FAR = \frac{\text{Number of imposter persons accepted as genuine}}{\text{Total number of persons outside the database}} \tag{11}$$

**b. False Rejection Rate (FRR)**

The test image from the data set is not matched with the images in the data set and can be calculated using Equation 12.

$$FRR = \frac{\text{Number of genuine persons in the database rejected}}{\text{Total number of persons inside the database}} \tag{12}$$

**c. Equal Error Rate (EER)**

It is the juncture value of FRR and FAR in the graph.

**d. Recognition Rate (RR)**

The number of legal persons successfully matched in the data set and is given by Equation 13.

$$TSR = \frac{\text{Number of the genuine persons recognized correctly}}{\text{Total number of the persons inside the database}} \quad (13)$$

e. *Maximum RR (MRR)*

The maximum value of RR.

f. *Optimum RR (ORR)*

The RR value corresponding to EER value.

**B Implementation and Experimental Result Analysis**

The face datasets viz., JAFFE, L-SPACEK, YALE and ORL are used to examine the proposed model by measuring performance metrics. The total number of persons in the dataset are clustered into two as Persons Inside Database (PID) and Persons Outside Database (POD) to compute FRR and FAR for the measurement of percentage RR

**a. Result Investigation using JAFFE DataSet**

The total number of persons in this dataset are ten with twenty images per person. The performance metrics such as percentage FRR, FAR, and TSR are calculated for variations in threshold values and the graphs are plotted. The variations of FRR, FAR and TSR obtained for deviations in PID with constant POD are shown in Figures 7, 8 and 9 for combinations of 4:4, 5:4, 6:4 respectively. The variations of FRR, FAR and TSR obtained for constant PID with deviations in POD are shown in Figures 10, and 11 for combinations of 5:4, and 6:4 respectively. It is witnessed that the values of FRR decrease with increase in threshold values, whereas, the values of FAR and TSR increases with threshold values.

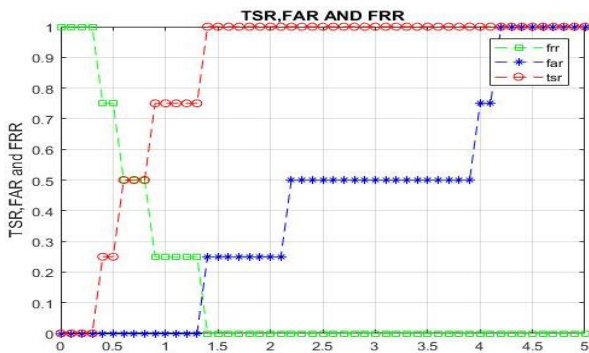


Figure.7 Variations of performance parameters for PID and POD of 4:4 combinations.

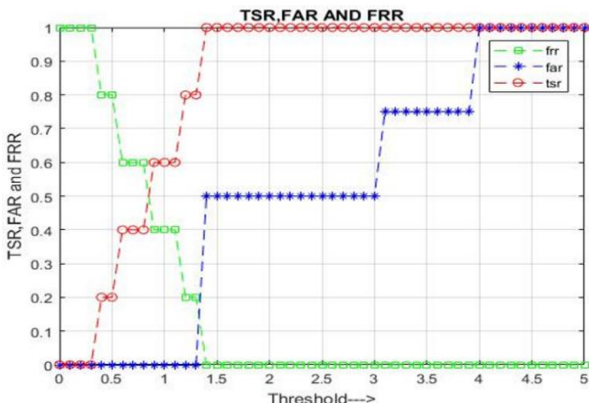


Figure. 8 The result deviations for 5:4 combination of PID and POD.



Figure. 9 The result deviations for 6:4 combination of PID and POD

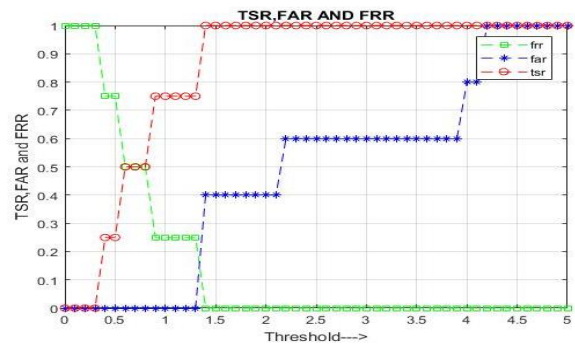


Figure. 10 The result deviations for 4:5 combinations of PID and POD

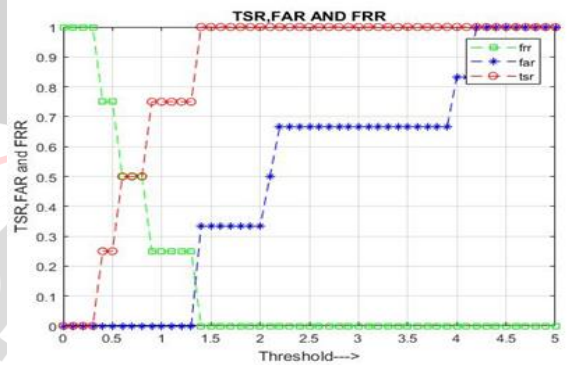


Figure. 11 The result deviations for PID and POD of 4:6 combinations.

The values of percentage EER, OTSR and MTSR for dissimilar PID and POD mixtures are prepared at table 1. It is witnessed that, values of percentage OTSR rise with rise in values of PID and percentage MTSR values constant at 100.

Table 1. Deviations of result METRICS with PID and POD for JAFFE Database

PID	POD	%EER	%OTSR	%MTSR
4	4	15	75	100
5	4	14	80	100
6	4	12	84	100
4	5	15	75	100
4	6	12	75	100

**b. Result Investigation using L-SPACEK Dataset**

The total numbers of persons in this dataset are one hundred fifty-two with twenty images per person. The parameters viz., FRR, FAR, and TSR are calculated for deviation thru values of threshold and are plotted. The variations of FRR, FAR and TSR obtained with deviations in PID and constant POD are shown in Figures 12, 13 and 14 for combinations of 40:60, 50:60, 60:60 correspondingly. The deviations of percentage FRR, FAR and TSR obtained for constant PID with deviations in POD are shown in Figures 15, and 16 for combinations of 60:40, and 60:50, correspondingly. The

observed FRR values decline thru rise in the values of threshold while, the FAR and TSR values rise thru rise in the values of threshold. The values of TSR is constant at 100% of the threshold values between 0.6 and 1.2, whereas for the threshold values of less than 0.6, TSR values decreases from 100% to 0%. For higher values of threshold, the TSR values remain constant, but the values of FAR increases from 0% to 100%, which is a limitation.

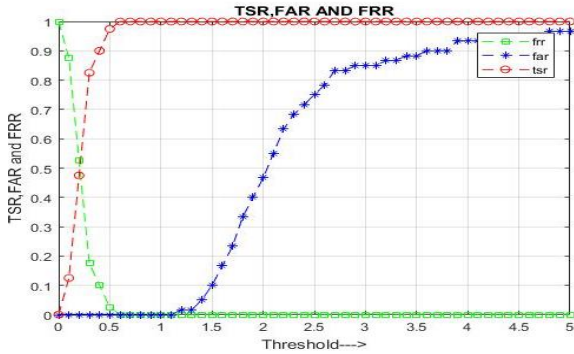


Figure. 12 The result deviations for 40:60 combination of PID and POD

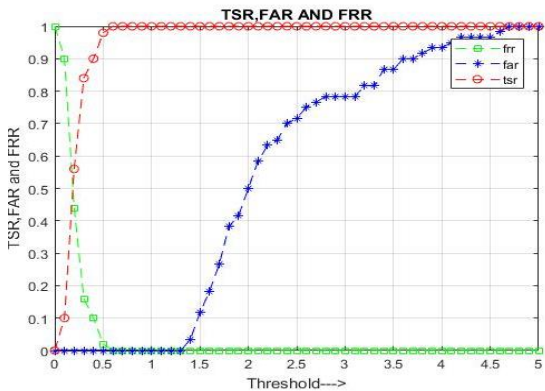


Figure.13 The result deviations for 50:60 combinations of PID and POD

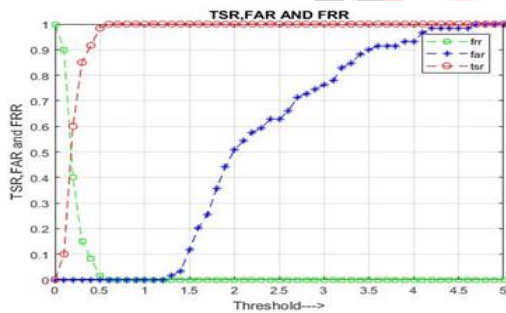


Figure. 14 The result deviations for 60:60 combinations of PID and POD

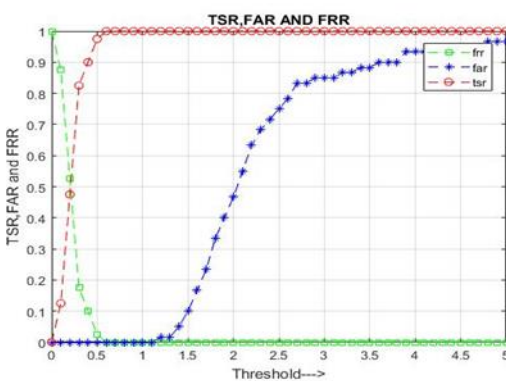


Figure.15 The result deviations for 60:40 combinations of PID and POD

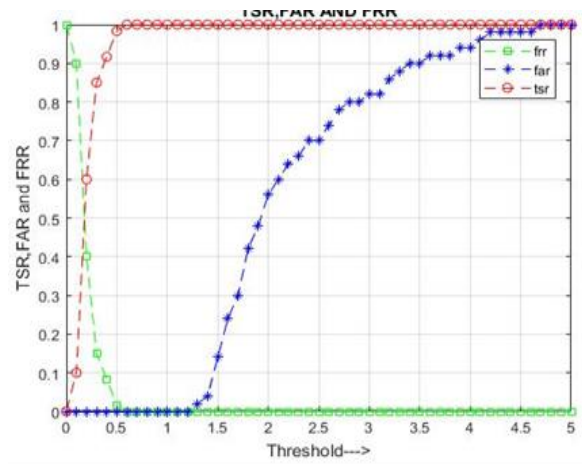


Figure.16 The result deviations for 60:50 combination of PID and POD

The deviations in the values of EER, OTSR and MTSR for dissimilar PID and POD amalgamations are organized in Table 2.

Table 2. The result constraints with different PID and POD combinations for L-SPACEK.

PID	POD	%EER	%OTSR	%MTSR
40	40	0	99	100
40	50	0	99	100
40	60	0	98	100
50	60	0	99	100
60	59	0	99	100

The calculated EER, OTSR and MTSR percentage values remains almost constant at 0, 99 and 100 aimed at the different PID and POD mixtures for threshold values between 0,6 and 1.2. For higher values of threshold, the percentage MTSR is 100%, which is an advantage, however the values of percentage FAR increases to 100% which is most undesirable condition.

c. Result Investigation using YALE Dataset

The total number of persons in this dataset are fifteen with eleven images per person. The calculated outcome of percentage FRR, FAR, and TSR for variations in threshold values are plotted in the graphs. The deviations of FRR, FAR and TSR obtained for deviations in PID with constant POD are shown in Figures 17, 18 and 19 for combinations of 8:5, 9:5, 10:5 correspondingly. The deviations of FRR, FAR and TSR obtained aimed at constant PID with deviations in POD are shown in Figures 20, and 21 for combinations of 8:6, and 8:7, correspondingly. It is witnessed that the values of FRR decline thru rise in the values of threshold while, the FAR and TSR values rise thru rise in the values of threshold. The TSR values are constant at 100% of the threshold values more than 2, and TSR values decrease from 100% for threshold values less than 2. For higher values of threshold, the TSR values remain constant and high, but the values of FAR increases from 0% to 100%, which is a limitation.

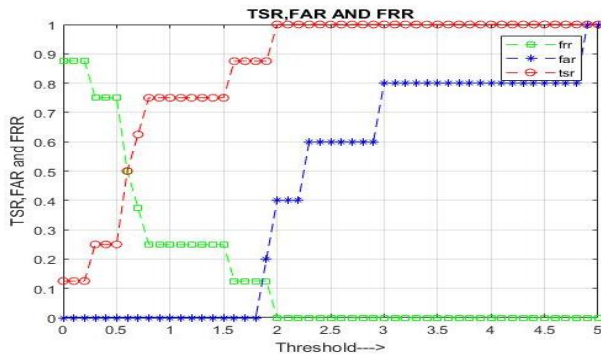


Figure.17 The result deviations for 8:5 combination of PID and POD

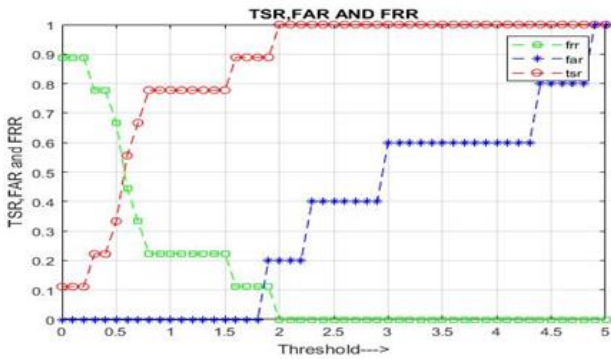


Figure.18 The result deviations for 9:5 combination of PID and POD

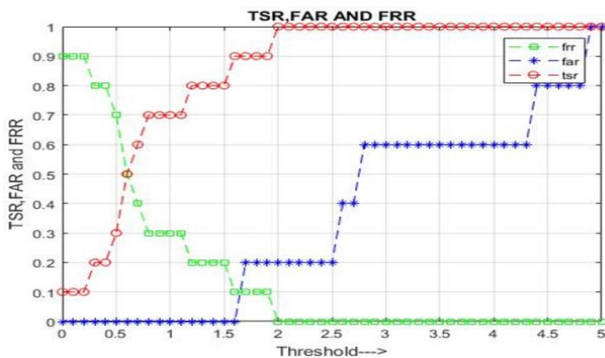


Figure.19 The result deviations for 10:5 combination of PID and POD

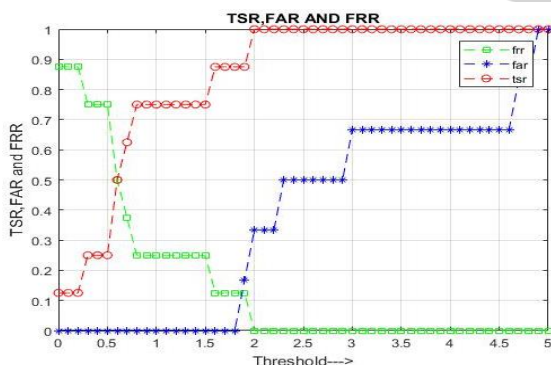


Figure. 20 The result deviations for 8:6 combination of PID and POD

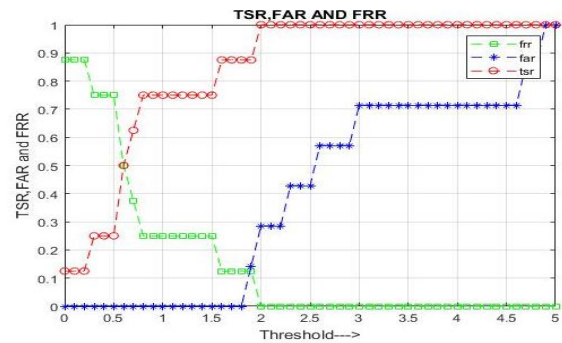


Figure. 21 The result deviations for 8:7 combination of PID and POD

The percentage values of EER, OTSR and MTSR for different PID and POD combinations are organized in Table 3. It is witnessed that, the percentage values of EER, and OTSR remains constant at 12, and 88 for the variations in POD and constant PID combinations of threshold values nearer to 1.9. For threshold values more than 2, the percentage MTSR is 100%, which is an advantage, however the values of percentage FAR rises with a rise in threshold to 100% which is most undesirable condition.

Table 3. The result constraints with different PID and POD combinations for YALE

PID	POD	%EER	%OTSR	%MTSR
8	5	12	88	100
8	6	12	88	100
8	7	12	88	100
9	5	11	89	100
10	5	10	90	100

d. Result Investigation using ORL Dataset

The entire dataset consists of 40 distinct persons with 10 different images per person. The performance metrics viz., FRR, FAR, and TSR are calculated for deviations in the values of threshold and plotted in the diagrams. The deviations of FRR, FAR and TSR obtained for deviations in PID with constant POD are shown in Figures 22, 23 and 24 for combinations of 10:10, 20:10, 30:10 correspondingly. The deviations of FRR, FAR and TSR obtained for constant PID with deviations in POD are shown in Figures 25, and 26 for combinations of 10:20, and 10:30, correspondingly. The values of FRR decline with a rise in the values of threshold while, the FAR and TSR values rise thru values of threshold. The TSR value is constant at 100% of the threshold values from 2.1, whereas for the threshold values of less than 2.1, TSR values decreases from 100% to 0%. For higher values of threshold, the TSR values remain constant at high, but the values of FAR increases from 0% to 100%, which is a limitation.

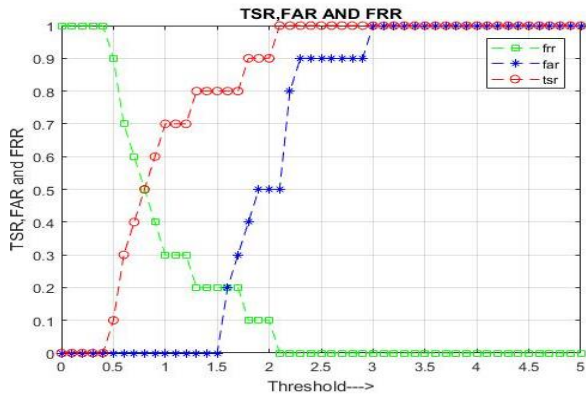


Figure.22 The result deviations for 10:10 combination of PID and POD for ORL dataset

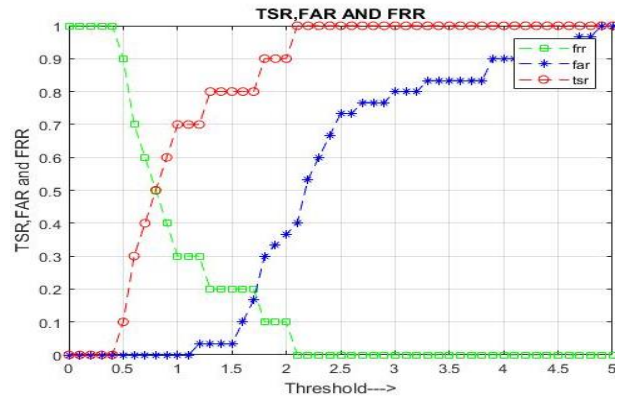


Figure.26 The result deviations for 10:30 combination of PID and POD for ORL dataset

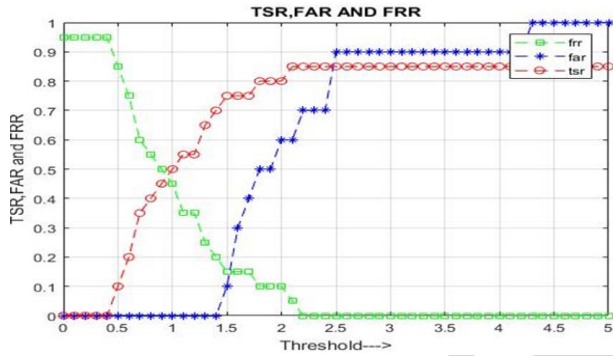


Figure.23 The result deviations for 20:10 combination of PID and POD for ORL dataset

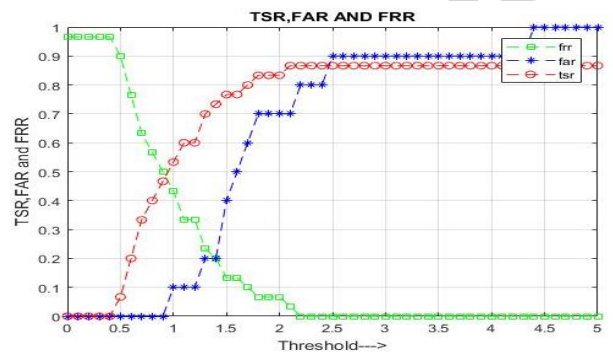


Figure.24 The result deviations for 30:10 combination of PID and POD for ORL dataset

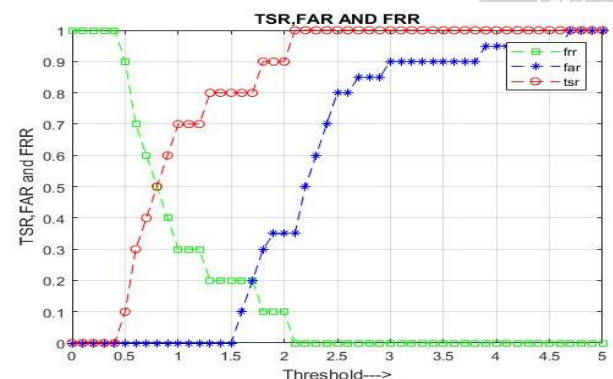


Figure.25 The result deviations for 10:20 combination of PID and POD for ORL dataset

The discrepancies of percentage values of EER, OTSR and MTSR for dissimilar PID and POD mixtures are organized in Table 4. The percentage EER, and OTSR values are almost constant at 20, and 80 for the variations in POD and constant PID combinations of threshold values around 1.7. For threshold values more than 2.2 with constant PID at 10, the percentage MTSR is 100%, which is an advantage, however the values of percentage FAR rises with a rise in threshold to 100% which is the most undesirable condition.

Table 4. The result constraints with different PID and POD combinations for ORL

PID	POD	%EER	%OTSR	%MTSR
10	10	20	80	100
10	20	20	80	100
10	30	18	80	100
20	10	15	75	85
30	10	20	74	86

C Comparison of results using different face datasets

The performance metrics EER and OTSR are noted corresponding to threshold values using L- Spacek, YALE, JAFFE and ORL face datasets are given Table 5. It is noticed that for less threshold value, the quarry face images are matched with dataset face images (prestored) and found EER and OTSR are zero and 99% respectively for L-Spacek dataset since the variations in face images of individual person are very less. The threshold values required are high for face datasets viz., YALE, JAFFE, and ORL for matching between query and dataset images. The average EER values are high, whereas the average OTSR values are low since the pose and other variations in face images of each person are high.

Table 5. Comparison of results for different datasets

Metrics	Face Datasets			
	L-Space k	YALE	JAFFE	ORL
Average Threshold	0.5	1.8	1.4	1.75
% Average EER	0	11.4	13.5	19
% Average OTSR	99	89	77.5	77.8

D Comparison of Projected Technique with Current Techniques

The percentage MTSR using ORL, YALE and JAFFE face datasets of projected technique is related to current

approaches obtainable by Erhu Zhang et al., [35], Shailaja and Anuradha [36], and Yubo Wang et al., [37] is shown in Table 6. The comparison revealed that % MTSR is improved in the case of projected technique related to current approaches.

**Table 6. %MTSR Comparison of Projected Technique with Current Approaches**

Methods	%MTSR		
	ORL dataset	YALE dataset	JAFFE dataset
Erhu Zhang et al.,[35]	74.06	80.77	-----
Shailaja and Anuradha[36]	87	92.8	-----
Yubo Wang et al.,[37]	----	-----	92.4
Projected method	94.2	100	100

## VI. CONCLUSION

A Convolution of Hybrid Domain Features for Human Recognition from Face Images is proposed in this paper. The face images of different face databases with different dimensions are converted into a uniform form dimension of 128x128. The DWT is applied to compress and remove noise in face images by considering low frequency coefficients of LL band. The HOG are computed with normalization using L2-Norm from LL band which resulted in cascade connection of DWT and HOG. The LL band matrix of size 64x64 is fused with HOG reshaped matrix of 42x42 using convolution technique results in efficient and robust final features of face images. The technique ED is used to measure result constraints. It is noticed that the proposed technique overtakes the existing approaches of face recognition. In future Deep learning techniques can be used in the place of ED to compare large image datasets.

## REFERENCES

[1] B. Miller, "Vital Signs of Identity," IEEE Spectrum, vol 31, issue 2, pp 22-30, 1994.

[2] G. Lawton, "Biometrics: A New Era in Security," Industry Trends, IEEE Computer, vol 31, pp16-18, 1998.

[3] A. Jain, R. Bolle and S. Pankanti, Biometrics: Personal Identification in Networked Society, Kluwer Academic Publishers, 1999

[4] D. Zhang, Automated Biometrics Technologies and Systems, Kluwer Academic Publishers, 2000

[5] E. C. Titchmarsh, Introduction to the Theory of Fourier Integral, Oxford University Press, NY, 1948

[6] Steven W. Smith, in Digital Signal Processing: A Practical Guide for Engineers and Scientists, Science Direct, 2003.

[7] J. W. Cooley, P. A. W. Lewis and P. D. Welch, "Historical Notes on the Fast Fourier Transform," IEEE Transactions on Audio and Electroacoustics, Vol 15, issue2, pp 76-79,1967.

[8] J. W. Cooley, P. A. W. Lewis and P. D. Welch, "Application of the fast Fourier transform to computation of Fourier integrals," IEEE Transactions on Audio and Electroacoustics, Vol 15, issue2, pp 79-84,1967.

[9] Vladimir Britanak, Patrick C. Yip and K.R. Rao, Discrete Cosine and Sine Transforms General Properties, Fast Algorithms and Integer Approximations, ScienceDirect, 2006

[10] Ali N. Akansu, and Richard A. Haddad, in Multiresolution Signal Decomposition (Second Edition), ScienceDirect, 2001

[11] X. Han, Q. Liu, J. Xu and H. Chen, "Face Recognition using Pearson Correlation and HOG with Single Training Image Per Person," IEEE

Conference on Chinese Automation Congress (CAC), pp. 3294-3298, 2018.

[12] G. G. Rajput, Prashantha and B. Geeta, "Face Photo Recognition from Sketch Images using HOG Descriptors," IEEE Second International Conference on Inventive Communication and Computational Technologies (ICICCT), pp. 555-558, 2018.

[13] Z. Xie, P. Jiang and S. Zhang, "Fusion of LBP and HOG using multiple kernel learning for infrared face recognition," IEEE/ACIS International Conference on Computer and Information Science (ICIS), pp. 81-84, 2017.

[14] M. Ghorbani, A. T. Targhi and M. M. Dehshibi, "HOG and LBP: Towards a Robust Face Recognition System," IEEE Tenth International Conference on Digital Information Management (ICDIM), pp. 138-141, 2015.

[15] H. Wang, D. Zhang and Z. Miao, "Fusion of LDB and HOG for Face Recognition," IEEE 37th Chinese Control Conference (CCC), pp. 9192-9196, 2018.

[16] H. T. M. Nhat and V. T. Hoang, "Feature Fusion by using LBP, HOG, GIST Descriptors and Canonical Correlation Analysis for Face Recognition," IEEE 26th International Conference on Telecommunications (ICT), pp. 371-375, 2019.

[17] B. H. Prasetyo, H. Tamura and K. Tanno, "The Facial Stress Recognition Based on Multi-Histogram Features and Convolutional Neural Network," IEEE International Conference on Systems, Man, and Cybernetics (SMC), pp 881-887, 2018.

[18] C. Jain, K. Sawant, M. Rehman and R. Kumar, "Emotion Detection and Characterization using Facial Features," IEEE 3rd International Conference and Workshops on Recent Advances and Innovations in Engineering (ICRAIE), pp. 1-6, 2018.

[19] P Rangsee, K B Raja and K R Venugopal, "Nibble-Based Face Recognition using Convolution of Hybrid Features," IEEE International Conference on Imaging, Signal Processing and Communication (ICISPC), Singapore, pp. 112-116, 2019.

[20] Zhao Lihong, Tian Yanan and Zhang Xili, "Face Recognition based on Wavelet and Fourier Transform," IEEE Chinese Control and Decision Conference, pp. 4225-4229, 2008.

[21] V. Espinosa-Duro and E. Monte-Moreno, "Face Recognition Approach based on Wavelet Transform," 42nd Annual IEEE International Carnahan Conference on Security Technology, pp. 187-190, 2008.

[22] V. Atamuradov, A. Eleyan and B. Karlik, "Performance Evaluation for Face Recognition using Wavelet-based Image De-noising," IEEE The International Conference on Technological Advances in Electrical, Electronics and Computer Engineering (TAECE), pp. 284-287, 2013.

[23] Z B Lahaw, D Essaidani and H Seddik, "Robust Face Recognition Approaches using PCA, ICA, LDA Based on DWT, and SVM Algorithms," IEEE 41st International Conference on Telecommunications and Signal Processing (TSP), pp. 1-5, 2018.

[24] Micheal J Lyons, "The Japanese Female Face Expression (JAFFE) Database", 1998, <http://www.karls.org/jaffe.html>.

[25] L-spacek database <http://cswww.essex.ac.uk/mv/allfaces>.

[26] Yale University, "The Yale Face Database", 1997", <http://cvc.cs.yale.edu/cvc/projects/yalefaces/yalefaces.html>

[27] AT&T Laboratories Cambridge, "The ORL Database of Faces", 1994, <http://www.cl.cam.ac.uk/research/dtg/atractive/face database.htm>.

[28] Multi-resolution Analysis: Discrete Wavelet Transforms, [https://nptel.ac.in/content/storage2/courses/117105083/pdf/ssg\\_m4112.pdf](https://nptel.ac.in/content/storage2/courses/117105083/pdf/ssg_m4112.pdf).

[29] N. Dalal and B. Triggs, "Histograms of Oriented Gradients for Human Detection," IEEE Computer Society Conference on Computer Vision and Pattern Recognition, pp 886-893, 2005.

[30] N. Dalal and B. Triggs, "Human Detection using Oriented Histograms of Flow and Appearance", Springer-Verlag, LNCS European Conference on Computer Vision, pp 428-441, May 2006.

[31] HOG:Computation <https://www.learnopencv.com/histogram-of-oriented-gradients/>

[32] S. A. Korkmaz, A. Akçiçek, H. Bınoł and M. F. Korkmaz, "Recognition of the stomach cancer images with probabilistic HOG feature vector histograms by using HOG features," IEEE 15th International Symposium on Intelligent Systems and Informatics (SISY), pp. 339-342, 2017.

- [33] C M Rader, "Discrete Convolutions via Mersenne Transforms," IEEE Transactions on Computers, vol. C-21, no. 12, pp. 1269-1273, December 1972.
- [34] Anton, Howard (2014), Elementary Linear Algebra (11th ed.), John Wiley & Sons. Erhu Zhang,
- [35] Yongchao Li and Faming Zhang, "A Single Training Sample Face Recognition Algorithm Based on Sample Extension", 2013 Sixth International Conference on Advanced Computational Intelligence, pp. 19-21, 2013.
- [36] K. Shailaja and B. Anuradha, "Effective Face Recognition using Deep Learning Based Linear Discriminant Classification", IEEE International Conference on Computational Intelligence and Computing Research, pp. 1- 6, 2016.
- [37] Yubo Wang, Haizhou AI, Bo WU and Chang Huang, "Real Time Facial Expression Recognition with Adaboost", IEEE International Conference on Pattern Recognition, pp. 926-929, 2004.

